Astro2020 APC White Paper

LiteBIRD: an all-sky cosmic microwave background probe of inflation

Project Area: Radio, Millimeter, and Submillimeter Observations from Space
Principal Author: Adrian T. Lee
Co-authors:

P. A. R. Ade[71], Y. Akiba[19,30], D. Alonso[71], K. Arnold[8], J. Aumont[44], J. Austermann[5], C. Baccigalupi[60,52,58], A. J. Banday[44], R. Banerji[66], R. B. Barreiro[68], S. Basak[49,60], J. Beall[5], S. Beckman[7], M. Bersanelli[63,55], J. Borrill[3,7], F. Boulanger[42], M. L. Brown[75], M. Bucher[38], A. Buzzelli[62], E. Calabrese[71], F. J. Casas[68], A. Challinor[74,72], V. Chan[37], Y. Chinone[7,18], J.-F. Cliche[34], F. Columbro[59,57], A. Cukierman[7], D. Curtis[7], P. Danto[40], P. de Bernardis[59,57], T. de Haan[3], M. De Petris[59,57], C. Dickinson[75], M. Dobbs[34], T. Dotani[15], L. Duband[39], A. Ducout[18], S. Duff[5], A. Duivenvoorden[70], J.-M. Duval[39], K. Ebisawa[15], T. Elleflot[8], H. Enokida[13], H. K. Eriksen[66], J. Errard[38], T. Essinger-Hileman[4], F. Finelli[53], R. Flauger[8], C. Franceschet[63,55], U. Fuskeland[66], K. Ganga[38], J.-R. Gao[65], R. Génova-Santos[67,69], T. Ghigna[76,18], A. Gomez[40], M. L. Gradziel[50], J. Grain[42], F. Grupp[48,47], A. Gruppuso[53], J. E. Gudmundsson[70], N. W. Halverson[9], P. Hargrave[71], T. Hasebe[15], M. Hasegawa[19,30], M. Hattori[31], M. Hazumi[19,15,18,30], S. Henrot-Versille[45], D. Herranz[68], C. Hill[7,3], G. Hilton[5], Y. Hirota[13], E. Hivon[41], R. Hlozek[37], D.-T. Hoang[1,77], J. Hubmayr[5], K. Ichiki[23], T. Iida[18], H. Imada[45], K. Ishimura[32], H. Ishino[26,19], G. C. Jaehnig[9], M. Jones[76], T. Kaga[15], S. Kashima[24], Y. Kataoka[26], N. Katayama[18], T. Kawasaki[20], R. Keskitalo[3], A. Kibayashi[26], T. Kikuchi[10], K. Kimura[27], T. Kisner[3], Y. Kobayashi[16], N. Kogiso[27], A. Kogut[4], K. Kohri[19], E. Komatsu[46], K. Komatsu[26], K. Konishi[14], N. Krachmalnicoff[60,52,58], C. L. Kuo[6,2], N. Kurinsky[6,2], A. Kushino[22], M. Kuwata-Gonokami[12], L. Lamagna[59,57], M. Lattanzi[54], A. T. Lee[7,3], E. Linder[3,7], B. Maffei[42], D. Maino[63,55], M. Maki[19], A. Mangilli[44], E. Martínez-González[68], S. Masi[59,57], R. Mathon[44], T. Matsumura[18], A. Mennella[63,55], M. Migliaccio[62,57], Y. Minami[19], K. Mistuda[15], D. Molinari[61], L. Montier[44], G. Morgante[53], B. Mot[44], Y. Murata[15], J. A. Murphy[50], M. Nagai[24], R. Nagata[19], S. Nakamura[33], T. Namikawa[74], P. Natoli[61,54], S. Nerval[37], T. Nishibori[17], H. Nishino[28], Y. Nomura[29], F. Noviello[71], C. O'Sullivan[50], H. Ochi[33], H. Ogawa[27], H. Ogawa[15], H. Ohsaki[13], I. Ohta[21], N. Okada[15], N. Okada[27], L. Pagano[61,54], A. Paiella[59,57], D. Paoletti[53], G. Patanchon[38], F. Piacentini[59,57], G. Pisano[71], G. Polenta[51], D. Poletti[60,52,58], T. Prouvé[39], G. Puglisi[6], D. Rambaud[44], C. Raum[7], S. Realini[63,55], M. Remazeilles[75], G. Roudil[44], J. A. Rubiño-Martín[67,69], M. Russell[8], H. Sakurai[12], Y. Sakurai[18], M. Sandri[53], G. Savini[73], D. Scott[36], Y. Sekimoto[15,19,30], B. D. Sherwin[74,72], K. Shinozaki[17], M. Shiraishi[25], P. Shirron[4], G. Signorelli[56], G. Smecher[35], P. Spizzi[40], S. L. Stever[18], R. Stompor[38], H. Sugai[18], S. Sugiyama[29], A. Suzuki[3], J. Suzuki[19], E. Switzer[4], R. Takaku[12], H. Takakura[11], S. Takakura[18], Y. Takeda[15], A. Taylor[76], E. Taylor[7], Y. Terao[13], K. L. Thompson[6,2], B. Thorne[76], M. Tomasi[63,55], H. Tomida[15], N. Trappe[50], M. Tristram[45], M. Tsuji[25], M. Tsujimoto[15], C. Tucker[71], J. Ullom[5], S. Uozumi[26], S. Utsunomiya[18], J. Van Lanen[5], G. Vermeulen[43], P. Vielva[68], F. Villa[53], M. Vissers[5], N. Vittorio[62], F. Voisin[38], I. Walker[71], N. Watanabe[20], I. Wehus[66], J. Weller[48,47], B. Westbrook[7], B. Winter[73], E. Wollack[4], R. Yamamoto[10], N. Y. Yamasaki[15], M. Yanagisawa[26], T. Yoshida[15], J. Yumoto[12], M. Zannoni[64,55], A. Zonca[8]

1. *Cornell Univ, USA*
2. *KIPAC, USA*
3. *LBNL, USA*
4. *NASA Goddard, USA*
5. *NIST, USA*
6. *Stanford Univ, USA*
7. *Univ of California, Berkeley, USA*
8. *Univ of California, San Diego, USA*
9. *Univ of Colorado, USA*
10. *AIST, Japan*
11. *Dept of Astronomy, Univ of Tokyo, Japan*
12. *Dept of Physics, Univ of Tokyo, Japan*
13. *GSFS, Univ of Tokyo, Japan*
14. *IPST, Univ of Tokyo, Japan*
15. *ISAS, JAXA, Japan*
16. *ISSP, Univ of Tokyo, Japan*
17. *JAXA, Japan*
18. *Kavli IPMU (WPI), Univ of Tokyo, Japan*
19. *KEK, Japan*
20. *Kitasato Univ, Japan*
21. *Konan Univ, Japan*
22. *Kurume Univ, Japan*
23. *Nagoya Univ, Japan*
24. *NAOJ, Japan*
25. *NITKC, Japan*
26. *Okayama Univ, Japan*
27. *Osaka Prefecture Univ, Japan*
28. *RESCEU, Univ of Tokyo, Japan*
29. *Saitama Univ, Japan*
30. *SOKENDAI, Japan*
31. *Tohoku Univ, Japan*
32. *Waseda Univ, Japan*
33. *Yokohama National Univ, Japan*
34. *McGill Univ, Canada*
35. *Three-Speed Logic, Inc., Canada*
36. *Univ of British Columbia, Canada*

37. *Univ of Toronto, Canada*
38. *APC, Univ Paris Diderot, France*
39. *CEA, France*
40. *CNES, France*
41. *IAP, Sorbonne Univ, France*
42. *IAS, Univ Paris-Sud, France*
43. *Institut Néel, France*
44. *IRAP, Univ de Toulouse, CNRS, CNES, UPS, France*
45. *LAL, Univ Paris-Saclay, France*
46. *MPA, Germany*
47. *MPE, Germany*
48. *Univ Sternwarte München, Germany*
49. *IISER-TVM, India*
50. *National Univ. of Ireland Maynooth, Ireland*
51. *ASI, Italy*
52. *IFPU, Italy*
53. *INAF – OAS Bologna, Italy*
54. *INFN Ferrara, Italy*
55. *INFN Milano, Italy*
56. *INFN Pisa, Italy*
57. *INFN Roma, Italy*
58. *INFN Trieste, Italy*
59. *Sapienza Univ of Rome, Italy*
60. *SISSA, Italy*
61. *Univ di Ferrara, Italy*
62. *Univ di Roma Tor Vergata, Italy*
63. *Univ of Milano, Italy*
64. *Univ of Milano Bicocca, Italy*
65. *SRON, Netherlands*
66. *Univ of Oslo, Norway*
67. *IAC, Spain*
68. *IFCA, CSIC-Univ de Cantabria, Spain*
69. *Univ de La Laguna, Spain*
70. *Stockholm Univ, Sweden*
71. *Cardiff Univ, UK*
72. *KICC, UK*

73. *Univ College London, UK*
74. *Univ of Cambridge, UK*
75. *Univ of Manchester, UK*
76. *Univ of Oxford, UK*
77. *USTH, Vietnam*

Executive Summary

The LiteBIRD mission will map polarized fluctuations in the cosmic microwave background (CMB) to search for the signature of gravitational waves from inflation, potentially opening a window on the Universe a fraction of a second after the Big Bang. CMB measurements from space give access to the largest angular scales and the full frequency range to constrain Galactic foregrounds, and LiteBIRD has been designed to take best advantage of the unique window of space. LiteBIRD will have a powerful ability to separate Galactic foreground emission from the CMB due to its 15 frequency bands spaced between 40 and 402 GHz and sensitive 100-mK bolometers. LiteBIRD will provide stringent control of systematic errors due to the benign thermal environment at the second Lagrange point, L2, 20-K rapidly rotating half-wave plates on each telescope, and the ability to crosscheck its results by measuring both the reionization and recombination peaks in the B-mode power spectrum. LiteBIRD would be the next step in the series of CMB space missions, *COBE*, *WMAP*, and *Planck*, each of which has given landmark scientific discoveries.

The 4,736 detectors are distributed between three 5-K cooled telescopes, called the Low-, Medium-, and High-frequency telescopes (LFT, MFT, and HFT), with 31 arc-min resolution at 140 GHz. LiteBIRD will map 20 times deeper than *Planck*, with a total error of $\delta r < 0.001$, conservatively assuming equal contributions of statistical error, systematic error, and margin. LiteBIRD will be designed to discover or disfavor the best motivated inflation models – single-field models that naturally explain the observed value of the spectral index of primordial density perturbations, with a characteristic scale of the potential comparable to or larger than the Planck scale. LiteBIRD will also measure the optical depth to reionization to cosmic-variance-limited error, enabling ground-based high-resolution CMB experiments to measure the sum of neutrino masses.

The proposed mission will be a partnership. Japan Aerospace Exploration Agency (JAXA) will provide the launch, spacecraft, Joule-Thomson coolers, LFT and its wave-plate. Europe will build the MFT and HFT, their waveplates, and the 100-mK cooler. Canada will contribute the 300-K detector readout electronics. The U.S. will build the detector arrays, cold readout electronics, and the 1.8-K cooler likely through a NASA mission of opportunity cost capped at $75M. In May 2019, JAXA selected LiteBIRD as a "strategic L-class" mission for launch in early 2028. The total mission cost is estimated to be approximately $500M, and therefore the U.S. contribution is highly leveraged. Finally, LiteBIRD technologies have been tested or will be tested in the near future on ground-based experiments.

LiteBIRD's ability to measure the entire sky at the largest angular scales with 15 frequency bands is complementary to that of ground-based experiments such as South Pole Observatory, Simons Observatory, and CMB-S4, which will focus on deep observations of low-foreground sky. LiteBIRD can provide valuable foreground information for ground-based experiments and ground-based experiments can improve LiteBIRD's observations with high-resolution lensing data.

A Key Science Goals and Objectives

CMB measurements provide a unique probe of fundamental physics and the origin and evolution of structure in the Universe. Observations of CMB temperature fluctuations have played a pivotal role in establishing the standard cosmological model and provide insights into the origin of structure, the density of baryons, dark matter, and dark energy, the number of neutrino species, and the global properties of spacetime. Many remaining questions about the Universe can best be answered through precise measurements of CMB polarization anisotropy. Observations of CMB polarization caused by density perturbations are already beginning to

refine constraints on the standard cosmological model. More significantly, a detection of CMB polarization generated by primordial gravitational waves would open an unexplored frontier of physics and shed light on processes that occurred even before the Universe became filled with a hot plasma of standard model particles. Characterization of this signal would provide access to fundamental physics at energies far beyond the reach of CERN's Large Hadron Collider, revolutionizing our understanding of physics and the early Universe.

LiteBIRD will survey the full sky and conduct a search for the imprint of gravitational waves more than 40 times more sensitive than current experiments. A detection of gravitational waves would provide a window to the primordial Universe, which leaves in its wake primordial density perturbations in radiation and matter that are the seeds for all the structure we see today. The results of the LiteBIRD mission will fulfill the NASA's Strategic Goal to "Expand scientific understanding of the Earth and the Universe in which we live." LiteBIRD would be the next step in the series of CMB space missions, *COBE*, *WMAP*, and *Planck*, each of which has given landmark scientific discoveries.

The leading paradigm for the generation of these primordial density perturbations is inflation[1, 2, 3, 4], a period of nearly exponential expansion of the Universe. This expansion not only generates density perturbations, but in addition creates gravitational waves. These gravitational waves persist and become imprinted in the CMB temperature and polarization anisotropies. Unlike density perturbations, the gravitational waves produce a polarization pattern with a curl component, commonly referred to as "B-mode" polarization. The amplitude of the signal is proportional to the expansion rate so that the strength of the B-mode signal would provide a measurement of the expansion rate during inflation. In addition, because general relativity relates the expansion rate to the energy density, a detection would allow us to infer one of the most basic properties of inflation, its energy scale.

The polarization pattern imprinted at the time of recombination peaks at degree angular scales (corresponding to multipoles of $\ell \simeq 80$). Even though density perturbations generate no intrinsic B-mode polarization, weak gravitational lensing converts the "E-mode" polarization they generate into B modes. This effect peaks on much smaller scales of a few arcminutes (corresponding to multipoles of $\ell \simeq 1000$). This contribution is well-understood theoretically, and LiteBIRD is sensitive to any excess over the lensing signal caused by the imprint of gravitational waves. In addition, B-mode polarization can be produced on larger scales by the scattering of the gravitational-wave-induced quardupolar temperature anisotropy around electrons in the reionizing Universe. This signal is dominant on large angular scales (corresponding to $\ell \simeq 10$) where B modes from lensing are subdominant, providing an additional signature.

As well as the B modes caused by weak gravitational lensing of E modes, there are additional sources of B-mode polarization at microwave frequencies. Thermal emission by interstellar dust grains that are aligned with the Galactic magnetic field and synchrotron emission from electrons spiraling in the Galactic magnetic field provide the dominant contributions. Fortunately, the frequency dependence of the primordial signal and foreground emission differ significantly so that multi-frequency observations allow us to disentangle the primordial and foreground contributions.

LiteBIRD will survey the full sky in 15 frequency bands from 40 to 402 GHz, with combined polarization sensitivity of 2 μK-arcmin and angular resolution of 31 arcmin (at 140 GHz). This broad frequency coverage and high-resolution spectral information provide a foreground subtraction capability that cannot be achieved from the ground. Furthermore, rapid polarization modulation, a densely linked observation strategy that can only be achieved from space, and the stable environment of an L2 orbit provide an unprecedented ability to control systematic errors, especially at the largest angular scales of $\ell < 10$. Taken together, the control of

foregrounds and systematic errors give LiteBIRD the ability to detect both the B-mode reionization bump at $\ell \simeq 4$ and the recombination bump at $\ell \simeq 80$, giving much higher confidence that a primordial signal has been uncovered. If a tentative detection of a signal is seen from a ground or balloon observatory, LiteBIRD will make a definitive statement on the detection of the signal and drastically improve the quantitative constraints on the physics of inflation. The forecast for LiteBIRD's ability to measure the primordial B-mode power spectrum is shown in figure A.1

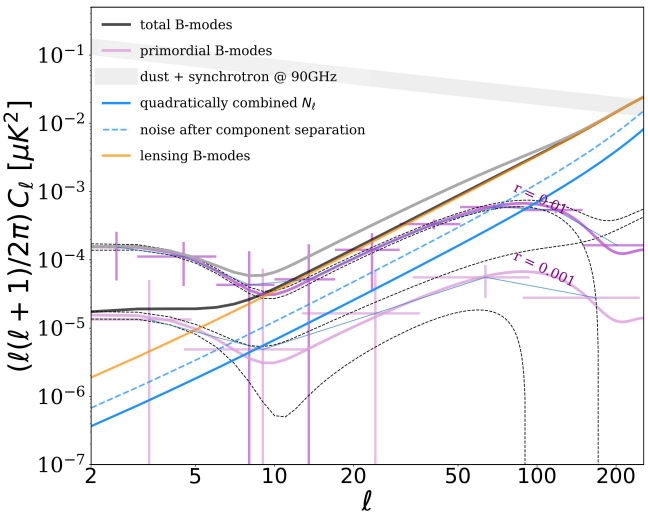

Figure A.1: CMB B-mode polarization power spectrum for tensor-to-scalar ratios $r = 0.001$ and $r = 0.01$. The gray and black curves show the sum of primordial B modes (purple) and lensing B modes (solid orange). Also shown are the noise levels for an optimal combination of the frequency channels (blue), the noise after component separation (dashed blue), and the total foreground power at 90 GHz over 60% of the sky. LiteBIRD is 40 times more sensitive to primordial B-mode polarization than current experiments after accounting for foreground removal. Unlike ground-based experiments, it can access the physics of both the reionization bump (at $\ell \simeq 4$) and the recombination bump (at $\ell \simeq 80$).

A detection of primordial gravitational waves with LiteBIRD would indicate that inflation occurred near the energy scale associated with grand unified theories, and would provide additional evidence in favor of the idea of the unification of forces. Additionally, the energy scale of inflation has important implications for other aspects of fundamental physics, such as axions and, in the context of string theory, the fields that control the shapes and sizes of the compact dimensions.

In the absence of a detection, LiteBIRD would provide upper limits on the amplitude of primordial gravitational waves that are almost two orders of magnitude stronger than current limits.There are only two classes of models that naturally explain the observed value of n_s and are consistent with current data. The two classes consist of models with potentials that (during inflation) are well approximated by a monomial, $V(\varphi) \simeq \mu^{4-p}\varphi^p$, and models in which the potential density $V(\varphi)$ approaches a plateau, either polynomially or exponentially over a characteristic scale M in field space. *To summarize,* LiteBIRD *is designed to discover or disfavor the best motivated inflation models, that is, all models in which the gravitational scale and the characteristic scale share a common origin, a class that includes the well-known Starobinsky model [5] and Higgs inflation [6].* Representative models and constraints achievable by LiteBIRD are shown in figure A.2

On the largest angular scales, the polarization anisotropies are generated by scattering of photons during the reionization epoch at $z \simeq 6$–10. The large-scale polarization anisotropies measured by LiteBIRD carry information on the nature of the epoch of reionization and will constrain models of the first stars. Beyond information about reionization itself, the optical depth to the surface of last scattering is a key parameter that currently limits any constraints that rely on comparisons of the amplitude of CMB anisotropies and clustering of the matter

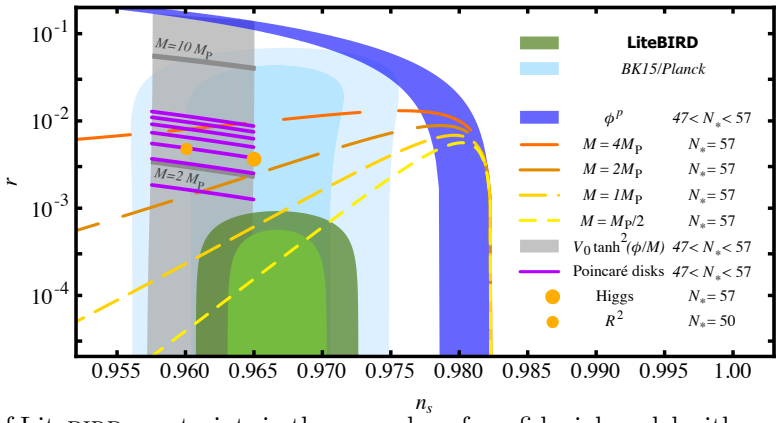

Figure A.2: Forecast of LiteBIRD constraints in the n_s–r plane for a fiducial model with $r = 0$. The lighter and darker shaded green regions show 68% and 95% confidence level upper limits. Also shown are representative individual models that can be detected by LiteBIRD (orange dots [5, 6] and purple lines [7, 8]) and the two classes of models that naturally predict the observed value of the scalar spectral index described in the text (blue band and orange lines [9]).

distribution, such as the measurement of the sum of neutrino masses. LiteBIRD will provide a cosmic-variance-limited measurement of E modes at low multipoles and will enable cosmological measurements of the sum of neutrino masses by high-resolution ground-based CMB experiments such as South Pole Observatory, Simons Observatory, and CMB-S4.

Furthermore, LiteBIRD's ability to measure the entire sky at the largest angular scales with 15 frequency bands is complementary to that of ground-based experiments which will focus on deep observations of low-foreground sky. LiteBIRD can provide valuable foreground information for ground-based experiments and ground-based experiments can improve LiteBIRD's observations with high-resolution lensing data. The LiteBIRD and CMB-S4 collaborations are exploring a Memorandum of Understanding to enable both experiments to enhance their reach using elements of the other's data.

Finally, the LiteBIRD all-sky polarized maps in 15 frequency bands will be a rich legacy data set for understanding the large-scale magnetic field structure in the Milky Way Galaxy, and have 5 times greater sensitivity to primordial magnetic fields than Planck.

In summary, the deliverables of the LiteBIRD mission are:

- an all-sky search for the fingerprints of inflation in the CMB sensitive to models in which inflation occurs at high energy and large field range;
- a cosmic-variance-limited measurement of the large-scale E-mode polarization, enabling cosmological measurements of the sum of neutrino mass, and improving the determination of when the Universe was reionized by the first stars;
- a full-sky map of dust and synchrotron polarization, giving measurements of the large-scale magnetic-field structure of the Milky Way.

We now turn to the two main challenges, foreground emission and control of systematic errors.

Foregounds The emission from our own Galaxy and extragalactic sources is collectively referred to as foreground emission. Diffuse polarized foreground emission is dominated by two components: synchrotron and thermal dust [10].

LiteBIRD's L1 goal is to achieve a total uncertainty in the tensor-to-scalar ratio parameter r of $\delta r < 10^{-3}$ including statistical and systematic uncertainties and equal budget of margin.

This goal requires removal of more than 99% of the polarized foreground emission from sky maps at frequencies near the foreground emission minimum, located at $\nu \approx 60 - 90$ GHz with a considerable scatter across the sky [11]. Figure A.3 shows the foreground emission in power-spectrum space. If not accounted for, Galactic polarized foregrounds result in a significant bias in r.

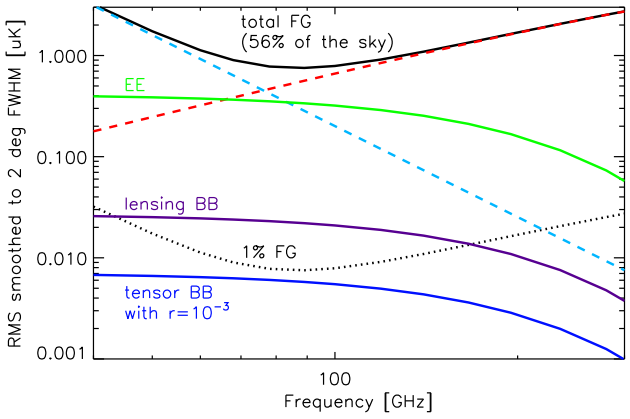

Figure A.3: RMS polarized intensity smoothed with a 2° beam, in units of antenna temperature. The cyan and red dashed lines show synchrotron and thermal dust emission, respectively. "EE," "lensing BB," and "tensor BB" show the RMS of E-mode polarization, B modes from lensing, and B modes from gravitational waves with LiteBIRD's target tensor-to-scalar ratio of $r = 10^{-3}$, respectively. The black solid line shows the sum of synchrotron and dust over 56% of the sky. The dotted line shows 1% of the black solid line.

Gravitational lensing also contributes to the statistical error of the B-mode power spectrum and the statistical uncertainty can be decreased by "delensing." Our baseline, however, is to achieve $\delta r < 10^{-3}$ *without* such a procedure, which, once implemented, will further increase our accuracy of the measurement of the primordial B-mode signal.

The LiteBIRD design is based on: (1) a wide frequency coverage to disentangle the CMB B-mode signal from the foreground components (see Figure A.3) and to minimize the foreground bias in r; and (2) sensitive detectors distributed optimally across frequency bands to minimize the effective noise after foreground removal.

Our baseline model of the foreground sky is the "d1s1" version of the "Python Sky Model" (PySM) [12]. PySM is a Python-based simulation software that provides a model of the sky emission at microwave frequencies based on the available information from *Planck* and *WMAP*. We generate 1000 realizations of the CMB (with no primordial tensor mode, i.e., $r_{\rm input} = 0$) and noise maps at `HEALPix`'s $N_{\rm side} = 64$, which corresponds to a pixel size of 0.91° on a side. Maps generated at this resolution safely support multipoles up to $2N_{\rm side} = 128$, which is smaller than our target maximum multipole of 200; thus, our results should be considered as conservative. This choice is justified also because, when $r \ll 10^{-2}$, most of the information on r *in the absence of delensing* (which is part of the L1 requirement) comes from the reionization bump at $\ell \lesssim 10$. The results are shown in Figure A.4. The average value of the uncertainty on r for a fiducial value of $r = 0$, $\sigma(r = 0)$, from 1000 realizations is $\langle\sigma(r = 0)\rangle = 0.58 \times 10^{-3}$ for $\tau = 0.0544$. We have also performed the analysis using different fitting technique such as the Bayesian method `Commander` [13], the template-based method [14], and the internal linear combination (ILC)-based method with needlets [10]. We find consistent answers to within the limitations and differences of the methods.

Systematic error study The control of systematic errors originating from the instrument, or imperfect modeling and correction of the data, is one of the primary drivers in the design of LiteBIRD. The main systematic error sources include: beam mismatches, largely in the far side-

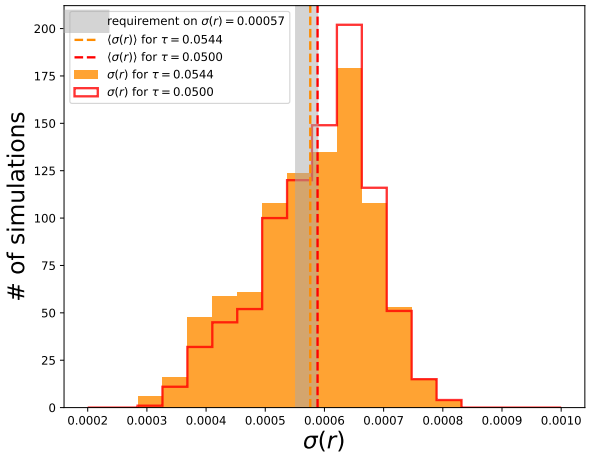

Figure A.4: Distributions of $\sigma(r = 0)$ obtained from 1000 realizations of the simulation including CMB, noise, and diffuse foreground emission. The filled orange histogram shows the distribution for $\tau = 0.0544$, while the red histogram shows that for $\tau = 0.05$. The dashed lines show the corresponding average values of $\sigma(r = 0)$.

lobes; instrumental polarization; imperfect polarization efficiency; gain variations; pointing errors; polarization angle error; correlated noise (for intensity estimation only using a half-wave plate, HWP); cosmic-ray glitches; bandpass errors; imperfect modeling of the transfer function; and detector system non-linearity. In total about 70 systematic sources have been identified. Errors have been propagated analytically and/or by simulation to the component separation methods to access the impact of residual foregrounds on the final B-mode spectra.

Table A.1: Contribution to the uncertainty on the tensor-to-scalar ratio

	δr
Stat. Error (FG subt.)	0.58×10^{-3}
Syst. error	0.71×10^{-3}
Total error	0.92×10^{-3}

In order to reduce spurious contamination of the Stokes polarization parameters LiteBIRD takes advantage of an L2-specific scanning strategy with relatively large precession angle giving a high level of redundancy of sky observations at many different timescales and a large-angle coverage for most of the pixels on the sky. This strategy has the advantage of reducing the level of intensity to polarization systematics, but also allows many different consistency tests. The use of an HWP, while significantly reducing the impact of $1/f$ noise in the polarization maps, also mitigates important systematic errors that were observed in *Planck* data, since it allows instantaneous estimation of Stokes parameters. Without an HWP, data from different detectors with potentially different properties would be differentiated potentially leading to intensity-to-polarization biases. The mitigated errors include the leakage induced by bandpass differences between detectors, beam and pointing mismatches, time-constant mismatches, and non-linearities (ADC non-linearities in the case of *Planck*).

The overall budget of systematic errors for the nominal LiteBIRD mission is presented in Table A.1. Quoted values are the contributions to δr of noise after component separation and of systematics, the two added in quadrature. We have adopted a conservative approach to account for the correlations of systematic error by applying a factor of 1.5 to the total δr obtained after combining all systematic errors.

The largest identified systematic error originates from far side-lobe pick up of the Galaxy. Figure A.5 shows the large contribution to the B-mode power spectrum of the far-sidelobe pickup. This systematic error can be mitigated by improving the telescope baffling and by modeling and subtraction of this spurious signal.

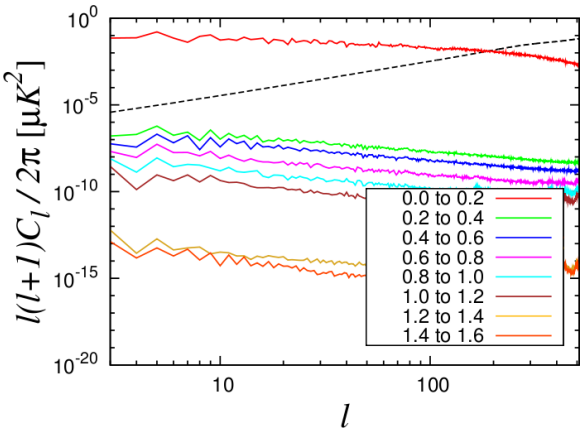

Figure A.5: Contributions to the B-mode signal of Galactic emission at 100 GHz seen through far side lobes over various angle ranges (in radians) with respect to the center of the beam. The Galactic plane has been masked using the WMAP P06 and *Planck* GAL060 joint mask. The dashed line is the lensing signal.[15, 16, 17]

B Technical Overview

Overall Experiment Design Japan, Europe, U.S. The LiteBIRD mission is based on a 5K-cooled crossed-Dragone 40-cm aperture telescope (LFT) and two 5K-cooled refractive telescopes with 30-cm (MFT) and 20-cm apertures (HFT) in an L2 sun-Earth Lissajous orbit. The observing strategy consists of a 0.05 RPM spin with telescope boresight offset 50 degrees from the spin axis along with a precession of the spin axis that gives one observation of the entire sky every 6 months. The entire sky is observed 6 times during the 3-year mission lifetime (baseline). LiteBIRD will be launched on an H3 rocket from Japan.

Nested octagonal V-grooves for passive radiative cooling and a pulse-tube cooler (ESA) provide a 20K-stage. The mechanical cryocoolers for lower temperature stages consist of a 4.8K-Joule Thompson (JT) cooler built by Sumitomo Heavy Industries (SHI) (flown on the Hitomi mission in 2016), a 1.8K-first-stage continuous adiabatic demagnetization refrigerator (ADR) (NASA-GSFC), and a 0.1K-second-stage continuous ADR (CNES).

The first optical element in each telescope is a continuously rotating Half-Wave Plate (HWP) which rotates the polarization of the incident CMB photons. The LiteBIRD modulator draws directly from the heritage of EBEX which flew such a unit during a long-duration balloon flight. The HWP will be radiatively cooled to the ambient 20K using a co-rotating absorptive collar. The HWP for LFT will incorporate an "achromatic" HWP with a stack of 5 sapphire plates to achieve the required bandwidth.

Scope of Mission of Opportunity The NASA Mission of Opportunity scope includes (i) three 100mK focal planes with antenna-coupled TES detectors for the LFT, MFT, and HFT, (ii) Cold readout electronics that multiplex in frequency domain (DfMUX), (iii) Isolating mechanical supports for the three focal plane, (iv) a GSFC-built 1.8K Adiabatic Demagnetization Refrigerator (ADR), and (v) participation in the collaboration-wide data analysis with deliverables in mission simulation.

Detector Focal Planes The three focal planes for the LFT, MFT, and HFT are depicted in B.7. The focal-plane modules have 9 different staggered frequency schedules to observe at 15 frequency bands to characterize foregrounds accurately.

The LFT and MFT will use broadband dual-polarized lenslet coupled sinuous antenna detector arrays. The detector architecture as shown in Figure B.8 has been developed at the University of California, Berkeley.[18] . The sinuous is a planar broadband polarization-sensitive antenna, and the contacting anti-reflection-coated lenslet increases forward gain of the antenna. On-chip bandpass filters partition the broadband RF signal into target frequency bands. Transition-Edge Sensor (TES) sensors on the bolometers are used to detect the RF power.

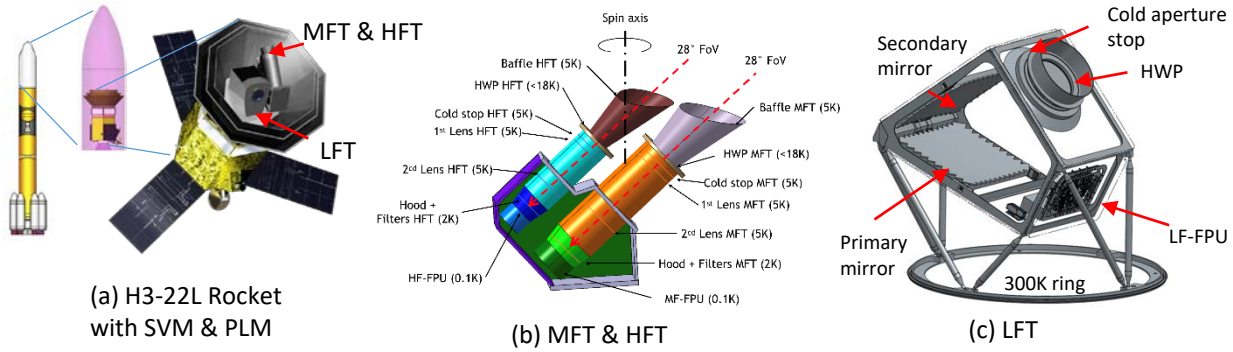

Figure B.6: Overview of the LiteBIRD mission.

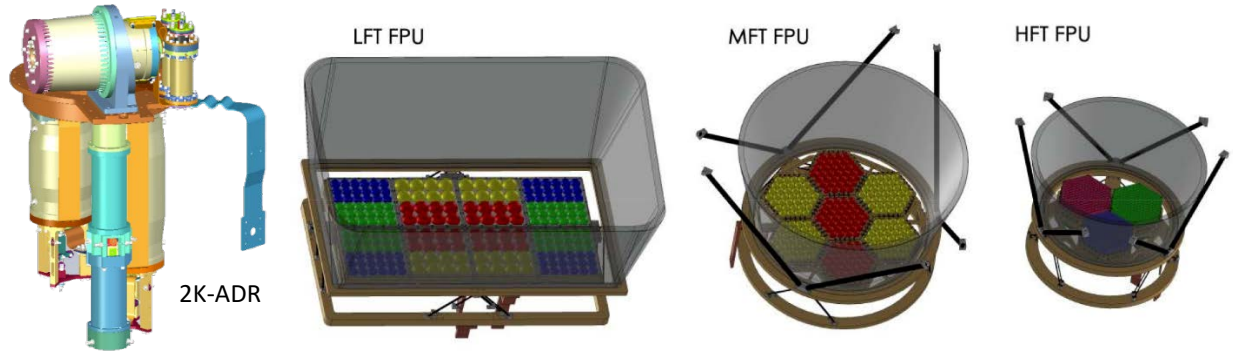

Figure B.7: Overview of the US Contributions to the LiteBIRD instrument, including the 2K-ADR, a three-stage ADR providing continuous cooling of the 2K stage, the focal planes associated with each of the telescopes, and the optical hoods shielding those focal planes.

The lenslet-coupled sinuous antenna detector was selected for LFT and MFT, since a trichroic pixel is required to achieve the required total sensitivity with the available focal plane area. The lenslet-coupled sinuous antenna detector is the only deployed Cosmic Microwave Background (CMB) detector that has demonstrated bandwidth beyond 2.3:1 which is required for a trichroic pixel with nominal single-band bandwidth. [19] The lenslet coupled sinuous antenna has deployed in POLARBEAR-2/Simons Array and South Pole Telescope Third Generation (SPT-3G). The Berkeley team developed the sinuous-based design for both experiments. POLARBEAR-2/Simons Array deployed a dichroic pixel that covers 90 GHz and 150 GHz simultaneously [20]. SPT-3G deployed trichroic pixel that covers 90 GHz, 150 GHz, and 220 GHz simultaneously [21].

The HFT will use orthomode transducer (OMT) coupled horn antenna detectors. The horn-coupled antenna detector was chosen for HFT for its maturity and the lower total sensitivity requirements in this frequency range. The horn-coupled antenna architecture has been developed at NIST [22]. Horns and waveguides are fabricated by stacking multiple layers of microfabricated silicon wafers with gold plate coating. The RF is then coupled by probe "fins" that extende into the waveguide. Similar to a lensle-coupled detector, the RF is partitioned into bands by on-chip filters then detected by TES sensors.

The horn-coupled technology has been used extensively in ground-based instruments such as ACT-pol, SPT-pol, and Advanced ACT [23, 24, 25]. The technology will soon be demonstrated in a balloon environment on the second flight of SPIDER, and has been selected as a detector technology for 90/150 GHz and 220/280 GHz frequency-band detectors for Simons Observatory [26, 27]. Advanced ACT deployed dichroic horn couple detector at 90/150 GHz [25]. Silicon

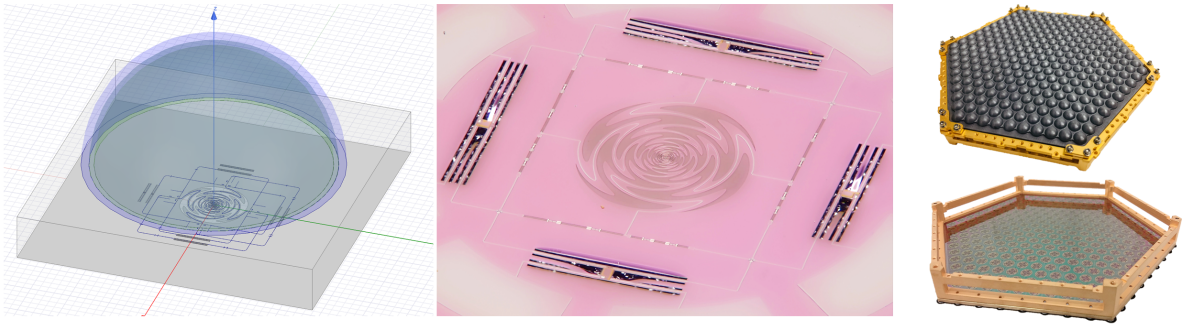

Figure B.8: (Left) simulation model of broadband anti-reflection coated lenslet coupled sinuous antenna detector. (Center) Microscope photograph of microfabricated sinuous antenna coupled detector. (Right) Machined monolithic silicon lenslet array and microfabricated detector array in gold plated detector holder from Berkeley.

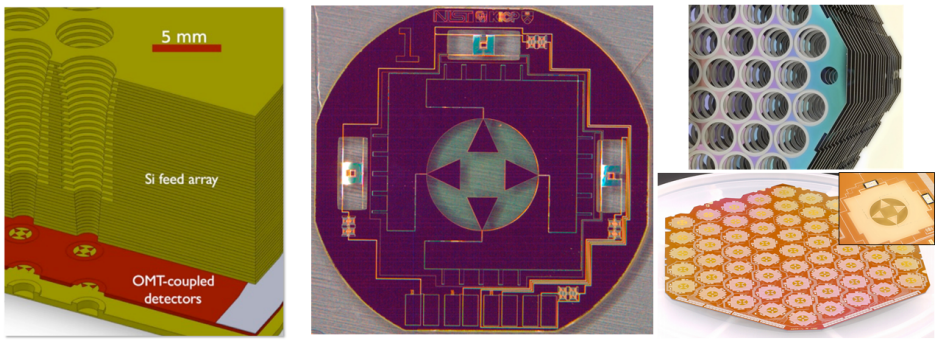

Figure B.9: (Left) Cross-section of horn coupled detector showing platelette horn array and OMT coupled detector wafer. (Center) Microscope photograph of microfabricated OMT coupled detector. (Right) Photograph of silicon platelette horn array and microfabricated OMT coupled detector array from NIST.

feedhorns and probe-coupled detectors have been demonstrated for the 280 GHz band by SPIDER [26], and no new fabrication tolerance challenges exist to scale to 400 GHz.

Cold Readout Electronics In the LiteBIRD implementation of the DfMUX system, 68 bolometers are connected to a single SQUID Array Amplifier (SAA) amplifier. The digital frequency-domain multiplexing (DfMux) readout system digitally generates a comb of sinusoidal bias carriers, one for each bolometer connected to the SAA. These signals are injected into the cryostat to provide the voltage bias carrier for each bolometer. Each detector operates in series with an inductor/capacitor (LC) resonator, and encodes the sky signal as an amplitude modulation of its bias carrier.

The DfMUX system has been successfully used in POLARBEAR-1 and the balloon-borne EBEX and is now operating in SPT-3G and the first receiver of the Simons Array. SPT-3G, in particular, has demonstrated the 68x multiplexer factor that will be used in LiteBIRD and has demonstrated detector-limited noise performance.

1.8 Kelvin Continuous Adiabatic Demagnetization Refrigerator The LiteBIRD instrument involves a series of refrigeration stages extending from room temperature to the focal planes at 100 mK. In the current mission formulation, the cryochain is divided as follows: 1) Pulse-tube cooler system provided by ESA and JT cryocoolers provided by JAXA will establish a base temperature of 4.5 K, 2) an ADR cooler supplied by GSFC will establish a lower temperature of approximately 1.8 K, and 3) an ADR provided by CEA will produce cooling at 300 mK and 100 mK for the focal planes. Under this proposal, NASA will provide a continuous 1.8K-ADR that will be the bridge between the CEA ADR and the JAXA JT cryocooler. The 1.8K ADR will use three ADR parallel stages, identical to one of the stages built for Astro-H,

to achieve continuous cooling at 1.8 K and to accommodate the periodic heat flows from the CEA ADR .

C Technology Drivers

As mentioned, all the detector and readout systems have been developed and tested in ground-based CMB experiments. For LiteBIRD, we have to adapt the ground-proven technologies for space flight. New developments include demonstrating robustness to launch vibration, survival of cosmic-ray irradiation, low-dead-time due to cosmic-ray events, and reduced saturation power compared to ground-based detectors. In terms of NASA-specific development, there are several technologies not currently at TRL-6 that will be demonstrated as TRL-6 before the PDR. Development of these technologies is currently being conducted by the LiteBIRD team, funded through a three-year NASA Technology Development (Tech-Dev) award.

Funding of that award starting in March of 2018, so the three year award duration will end in early 2021, at the time of the proposed CSR submission and the completion of Phase A. The deliverable of this Tech-dev award is advancing the LiteBIRD detector and cryogenic readout technologies to TRL-5. The development work during Phase B of this proposal is to then advance the technologies from TRL-5 to TRL-6.

D Organization, Partnerships, and Current Status

The LiteBIRD mission will be built under a partnership between Japan, Europe, Canada, and the United States. Japan will lead the L-class strategic JAXA mission with a scope that includes the launch and spacecraft. The European team is being formed, but elements being proposed include a leadership role by CNES, a ESA mission of opportunity and strong contributions from ESA member countries including the UK, Italy, and France. The Canadian team is in discussions with CSA. Masashi Hazumi is the PI of the JAXA mission, Ludovic Montier is the spokesperson of the European consortium, Matt Dobbs is the PI of the Canadian team, and Adrian Lee is the PI of the NASA mission of opportunity.

E Schedule

The global schedule will be driven by the JAXA mission schedule. The mission was approved by JAXA in May 2019 and the launch is planned for early 2028. The U.S. contribution is proposed as a NASA Mission of Opportunity that would begin Phase B (official start of mission work) in October of 2021.

F Cost

The JAXA main mission is cost capped at 300 Oku Yen (approximately $300M), and the U.S NASA Mission of Opportunity is cost capped at $75M. The European and Canadian contributions are not yet fully costed.

References

[1] Alexei A. Starobinsky. Relict Gravitation Radiation Spectrum and Initial State of the Universe. (In Russian). *JETP Lett.*, 30:682–685, 1979.

[2] A. H. Guth. Inflationary universe: A possible solution to the horizon and flatness problems. *Phys. Rev. D.* , 23:347–356, January 1981.

[3] A. D. Linde. A new inflationary universe scenario: A possible solution of the horizon, flatness, homogeneity, isotropy and primordial monopole problems. *Phys. Lett.*, B108:389–393, 1982.

[4] Andreas Albrecht and Paul J. Steinhardt. Cosmology for Grand Unified Theories with Radiatively Induced Symmetry Breaking. *Phys.Rev.Lett.*, 48:1220–1223, 1982.

[5] Alexei A. Starobinsky. A New Type of Isotropic Cosmological Models Without Singularity. *Phys.Lett.*, B91:99–102, 1980.

[6] Fedor L. Bezrukov and Mikhail Shaposhnikov. The Standard Model Higgs boson as the inflaton. *Phys. Lett.*, B659:703–706, 2008.

[7] Sergio Ferrara and Renata Kallosh. Seven-disk manifold, α-attractors, and B modes. *Phys. Rev.*, D94(12):126015, 2016.

[8] Renata Kallosh, Andrei Linde, Timm Wrase, and Yusuke Yamada. Maximal Supersymmetry and B-Mode Targets. *JHEP*, 04:144, 2017.

[9] Kevork N. Abazajian et al. CMB-S4 Science Book, First Edition. 2016.

[10] Planck Collaboration IV. Planck 2018 results. IV. Diffuse component separation. 2018.

[11] N. Krachmalnicoff et al. The S-PASS view of polarized Galactic Synchrotron at 2.3 GHz as a contaminant to CMB observations. 2018.

[12] Ben Thorne, Jo Dunkley, David Alonso, and Sigurd Naess. The Python Sky Model: software for simulating the Galactic microwave sky. *Mon. Not. Roy. Astron. Soc.*, 469(3):2821–2833, 2017.

[13] H. K. Eriksen, J. B. Jewell, C. Dickinson, A. J. Banday, K. M. Górski, and C. R. Lawrence. Joint Bayesian Component Separation and CMB Power Spectrum Estimation. Astrophys. J., 676:10–32, March 2008.

[14] Kiyotomo Ichiki, Hiroaki Kanai, Nobuhiko Katayama, and Eiichiro Komatsu. Delta-map method of removing CMB foregrounds with spatially varying spectra. *PTEP*, 2019(3):033E01, 2019.

[15] Hiroaki Imada, Tadayasu Dotani, Takashi Hasebe, Masashi Hazumi, Junji Inatani, Hirokazu Ishino, Shingo Kashima, Nobuhiko Katayama, Kimihiro Kimura, Tomotake Matsumura, Ryo Nagata, Yutaro Sekimoto, Hajime Sugai, Aritoki Suzuki, Shin Utsunomiya. The optical design and physical optics analysis of a cross-Dragonian telescope for LiteBIRD. *Proc. SPIE 10698, Space Telescopes and Instrumentation 2018*, 10698(10698K), July 2018.

[16] R. Nagata, H. Imada, H. Kanai, and LiteBIRD Phase A1 team. On the systematic effects of LiteBIRD observation XI. In *Spring Annual Meeting of Astronomical Society of Japan 2018*, March 2018.

[17] R. Nagata. Requirement analysis for LiteBIRD's optical system. *JAXA Supercomputer System Annual Report April 2017-March 2018*, JSS2 Inter-University Research, R17EACA34, August 2018.

[18] A. Suzuki. *Multichroic Bolometric Detector Architecture for Cosmic Microwave Background Polarimetry Experiments*. PhD thesis, University of California, Berkeley, 2013.

[19] Maximilian H. Abitbol, Zeeshan Ahmed, Darcy Barron, Ritoban Basu Thakur, Amy N. Bender, Bradford A. Benson, Colin A. Bischoff, Sean A. Bryan, John E. Carlstrom, and Clarence L. Chang. CMB-S4 Technology Book, First Edition. *arXiv e-prints*, page arXiv:1706.02464, Jun 2017.

[20] Yuki Inoue, P Ade, Y Akiba, C Aleman, K Arnold, C Baccigalupi, B Barch, D Barron, S Beckman, A Bender, D Boettger, J Borrill, S Chapman, Y Chinone, A Cukierman, T de Haan, M A Dobbs, A Ducout, R Dunner, T Elleflot, J Errard, G Fabbian, S Feeney, C Feng, G Fuller, A J Gilbert, N Goeckner-Wald, J Groh, G Hall, N Halverson, T Hamada, M Hasegawa, K Hattori, M Hazumi, C Hill, W L Holzapfel, Y Hori, L Howe, Y Inoue, F Irie, G Jaehnig, A Jaffe, O Jeong, N Katayama, J P Kaufman, K Kazemzadeh, B G Keating, Z Kermish, R Kaskitalo, T Kisner, A Kusaka, M Le Jeune, A T Lee, D Leon, E V Linder, L Lowry, F Matsuda, T Matsumura, N Miller, K Mizukami, J Montgomery, M Navaroli, H Nishino, H Paar, J Peloton, D Poletti, G Puglisi, C R Raum, G M Rebeiz, C L Reichardt, P L Richards, C Ross, K M Rotermund, Y Segawa, B D Sherwin, I Shirley, P Siritanasak, N Stebor, L Steinmetz, R Stompor, A Suzuki, O Tajima, S Takada, S Takatori, G P Teply, A Tikhomirov, T Tomaru, B Westbrook, N Whitehorn, A Zahn, and O Zahn. POLARBEAR-2: an instrument for CMB polarization measurements. *Astronomical Telescopes + Instrumentation*, 9914(55), 2016.

[21] B. Benson. The south pole telescope, 2013. Slides of a talk given at Cosmology after Planck Workshop, September 23 - 25, University of Michigan, Ann Arbor, MI. http://www.umich.edu/ mctp/SciPrgPgs/events/2013/CAP13/PresentationFiles/Benson.pdf.

[22] Johannes Hubmayr. Advances in Multichroic Feedhorn-Coupled TES Polarimeter Arrays for CMB Measurements. 2015.

[23] M. D. Niemack, P. A. R. Ade, J. Aguirre, F. Barrientos, J. A. Beall, J. R. Bond, J. Britton, H. M. Cho, S. Das, M. J. Devlin, S. Dicker, J. Dunkley, R. Dunner, J. W. Fowler, A. Hajian, M. Halpern, M. Hasselfield, G. C. Hilton, M. Hilton, J. Hubmayr, J. P. Hughes, L. Infante, K. D. Irwin, N. Jarosik, J. Klein, A. Kosowsky, T. A. Marriage, J. McMahon, F. Menanteau, K. Moodley, J. P. Nibarger, M. R. Nolta, L. A. Page, B. Partridge, E. D. Reese, J. Sievers, D. N. Spergel, S. T. Staggs, R. Thornton, C. Tucker, E. Wollack, and K. W. Yoon. ACTPol: A polarization-sensitive receiver for the Atacama Cosmology Telescope. *Proc. SPIE 7741, Millimeter, Submillimeter, and Far-Infrared Detectors and Instrumentation for Astronomy V*, 7714(771411S), Jun 2010.

[24] J. E. Austermann, K. A. Aird, J. A. Beall, D. Becker, A. Bender, B. A. Benson, L. E. Bleem, J. Britton, J. E. Carlstrom, C. L. Chang, H. C. Chiang, H. M. Cho, T. M. Crawford, A. T. Crites, A. Datesman, T. de Haan, M. A. Dobbs, E. M. George, N. W. Halverson,

N. Harrington, J. W. Henning, G. C. Hilton, G. P. Holder, W. L. Holzapfel, S. Hoover, N. Huang, J. Hubmayr, K. D. Irwin, R. Keisler, J. Kennedy, L. Knox, A. T. Lee, E. Leitch, D. Li, M. Lueker, D. P. Marrone, J. J. McMahon, J. Mehl, S. S. Meyer, T. E. Montroy, T. Natoli, J. P. Nibarger, M. D. Niemack, V. Novosad, S. Padin, C. Pryke, C. L. Reichardt, J. E. Ruhl, B. R. Saliwanchik, J. T. Sayre, K. K. Schaffer, E. Shirokoff, A. A. Stark, K. Story, K. Vanderlinde, J. D. Vieira, G. Wang, R. Williamson, V. Yefremenko, K. W. Yoon, and O. Zahn. SPTpol: an instrument for CMB polarization measurements with the South Pole Telescope. *Proc. SPIE 8452, Millimeter, Submillimeter, and Far-Infrared Detectors and Instrumentation for Astronomy VI*, 8452(84520E), Oct 2012.

[25] S. M. Duff, J. Austermann, J. A. Beall, D. Becker, R. Datta, P. A. Gallardo, S. W. Henderson, G. C. Hilton, S. P. Ho, J. Hubmayr, B. J. Koopman, D. Li, J. McMahon, F. Nati, M. D. Niemack, C. G. Pappas, M. Salatino, B. L. Schmitt, S. M. Simon, S. T. Staggs, J. R. Stevens, J. Van Lanen, E. M. Vavagiakis, J. T. Ward, and E. J. Wollack. Advanced ACTPol Multichroic Polarimeter Array Fabrication Process for 150 mm Wafers. *Journal of Low Temperature Physics*, 184(3):634–641, 2016.

[26] P. A. R. Ade et al. Antenna-coupled TES bolometers used in BICEP2, Keck array, and SPIDER. Astrophys. J., 812(2):176, 2015.

[27] Nicholas Galitzki, Aamir Ali, Kam S. Arnold, Peter C. Ashton, Jason E. Austermann, Carlo Baccigalupi, Taylor Baildon, Darcy Barron, James A. Beall, and Shawn Beckman. The Simons Observatory: instrument overview. 10708:1070804, Jul 2018.